Original Paper *Forma*, **25**, 31–35, 2010

Geometrical Optimization of Arrangement of Solar Cells in Photovoltaic Modules

Kei Obinata*, Naohiko Kato, Yasuhiko Takeda and Tomoyoshi Motohiro

Toyota Central R&D Laboratories, Inc., 41-1 Yokomichi, Nagakute-cho, Aichi 480-1192, Japan
**E-mail address: obinata@mosk.tytlabs.co.jp*

(Received May 6, 2010; Accepted November 4, 2010)

We have proposed that conversion efficiency of photovoltaic modules using thin film solar cells is significantly improved by optimizing the arrangement of each cell in the modules. When the cells are inclined with respect to the light-incident plane of the module, the module efficiency of the modules was relatively higher by 15–50% than the value for conventional arrangement. The module efficiency was further improved by grouping several inclined cells as a unit and optimally arranging the units, compared to uniform arrangements.
Key words: Photovoltaics, Solar Cells, Geometrical Optimization, Energy Conversion Efficiency, Short-Circuit Current Density

1. Introduction

Development of photovoltaic modules that provide both low cost and high conversion efficiency has been attracted much attention, as a renewable energy source to realize sustainable society. A cost of electricity as low as ¥10/kWh is needed for widespread use of photovoltaic systems. However, the cost is currently 2–3 times higher than the target value.

Photovoltaic modules using thin film solar cells (e.g., amorphous silicon cells, dye-sensitized cells and organic cells) are attractive candidates to reduce both the material cost and fabrication cost. However, they still have an issue of low conversion efficiency being around 10% or less (Green *et al.*, 2009). In the present study, we propose that module efficiency can be improved by optimally arranging the cells in a module.

The conversion efficiency is the product of the three factors: short-circuit current density, open circuit voltage, and filling factor. Among them, the short-circuit current density is characterized by optical absorbance and absorbed photon-to-electron conversion efficiency (APCE) as functions of the incident light wavelength. The issue that lowers the conversion efficiency of the thin film solar cells is the fact that the optical absorbance at around the absorption edge of the light-absorbing material used in the cells is quite low, although rather high values of APCE are maintained. As for dye-sensitized cells (DSCs), APCE was 80–95% at 400–600 nm and still over 60% at 600–700 nm (Fillinger and Parkinson, 1999). In contrast, the optical absorbance gradually decreases with increasing wavelength from around 600 nm, and is close to 0% at 850 nm, although it is sufficiently high at a shorter wavelength (Kusama *et al.*, 2007). Therefore, it is of the greatest importance to increase the optical absorbance of the modules, especially in the long wavelength range, to improve the conversion efficiency and to realize the high cost performance.

2. Arrangements of Solar Cells in Modules

When the optical absorbance of a cell is insufficient, the incident light is not completely absorbed but some portion goes through the cell in vain without contributing to photon-to-electron conversion (Fig. 1(a)). One of the methods to increase the absorbance is using a thicker cell. However, the longer propagation length of photo-generated carriers raises the recombination rate of the carriers, which would lower the conversion efficiency (Kao *et al.*, 2009).

Another method to increase the absorbance is to elongate the optical pass length by inclining the cells with respect to horizon, without changing the cell thickness (Fig. 1(b)). This does not elongate the propagation length of the carriers, and hence solves the recombination issue mentioned above.

The optical path length can be doubled by stacking two cells (Fig. 1(c)). Using mirrors at the side walls and the bottom further improves the absorbance, by reflecting the transmitted light back to the cells (Fig. 1(d)).

To examine the effect of the inclination and stacking of the cells mentioned above, the short-circuit current density of the modules using these arrangements were evaluated by both simulation and experiments. DSCs, which are intensively developed and close to practical uses, were employed here for the evaluation.

3. Simulation

3.1 Modeling with Monte Carlo simulation

The optical absorbance was calculated by simulating light propagation in the modules, based on a ray tracing using a Monte Carlo method. The short-circuit current density of the modules were obtained by integrating the product of the absorbance and the solar spectrum over the whole wavelength range, assuming APCE being 100%.

Figure 2 illustrates a typical structure of the modules consisting of several cells with the side and bottom mirrors. A two-dimensional model was used for simplification, assum-

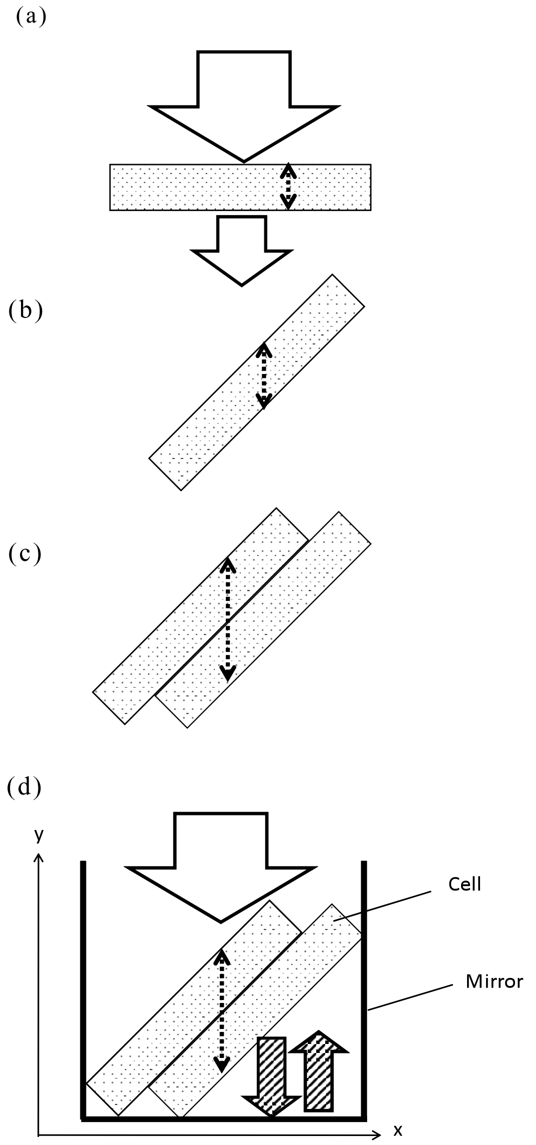

Fig. 1. Schematic diagram of arrangements of solar cells. Dotted rectangles: solar cells, white arrow: incident light, dashed arrow: optical path length, hatched arrows: transmitted and reflected light. (a) Horizontal arrangement. (b) Inclining arrangement. (c) Inclining with stacking. (d) Combination with side and bottom mirrors.

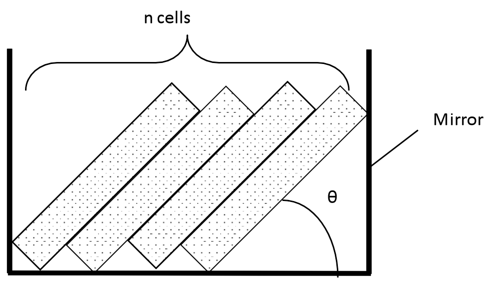

Fig. 2. Schematic diagram of a typical arrangement used for the simulation.

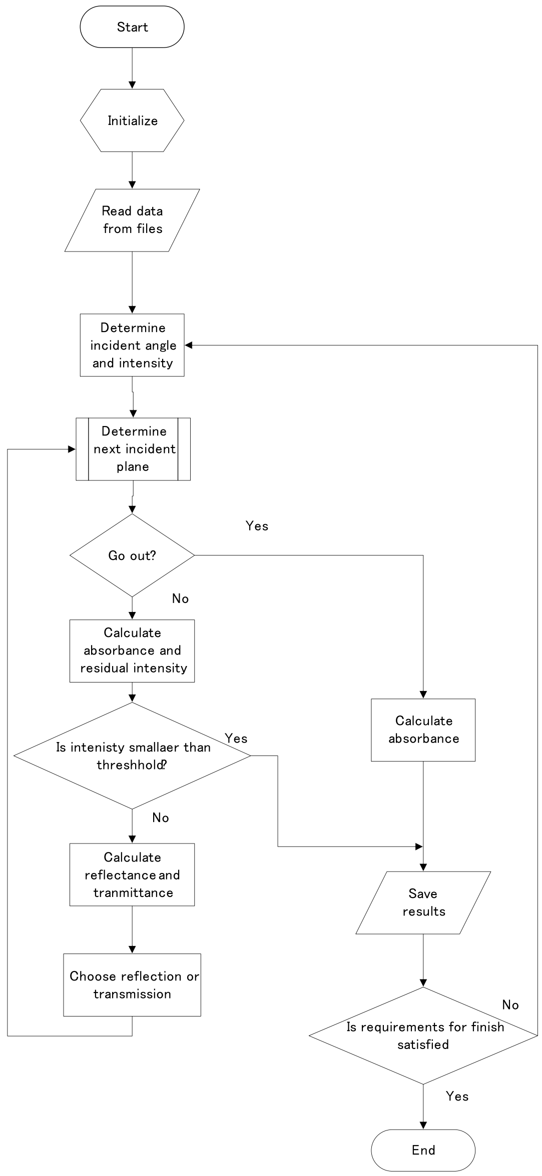

Fig. 3. Flowchart of the simulation program.

ing uniformity in z-direction.

The simulation program was developed using Visual-Basic 2008 (Microsoft corp.). The program flowchart is shown in Fig. 3. The accuracy of the internal valuables depends on the limitation of the digit number of the valuables. It was confirmed that the accuracy was sufficient in comparison with the accuracy of experimental data used in the simulation. Figure 4 shows a screenshot of the program.

3.2 Data used in the simulation

The input data for the simulation are optical constants of the materials used in the DSCs, cell sizes and solar spectrum. Optical constants were calculated from experimental data, as shown in Fig. 5. The cell size was set to equal to that in the experiments described in the next section. The AM1.5 spectrum, which is the standard of the solar spectrum and intensity on the surface of the earth (ASTM standard, direct+circumsolar of ASTM G173-03 Reference Spectra data from SMARTS v. 2.9.2 (NREL)) was used.

4. Experiments

4.1 Materials and structure of the cells

Nanopowder TiO_2 of 20 nm in average diameter, a red dye and an electrolyte containing I^-/I_3^- redox couples were

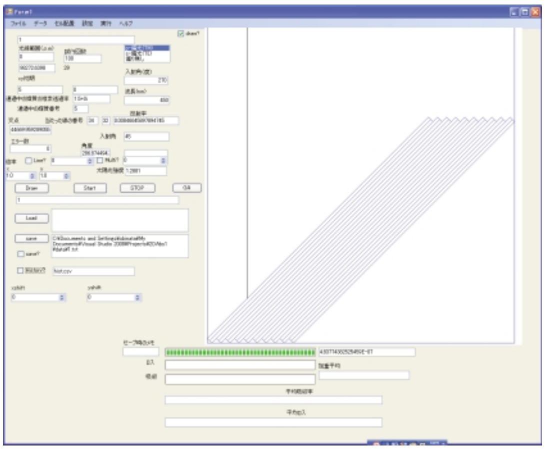

Fig. 4. Screenshot of the program. Each rectangle is a solar cell, and the black-colored line shows a ray trace.

used with SnO_2:F-covered glass plates to fabricate the DSCs. Detailed structure of the cells is the same as that used in the simulation model except for the peripheral seals.

4.2 Evaluation of the modules

The DSC modules of various arrangements similar to those used for the simulation (see Fig. 2) were composed using the cells mentioned above the side (only y-z planes) and bottom mirrors. Modules of the horizontal arrangement that are also equipped with mirrors on the both sides and the bottom were fabricated as the standard.

Current-voltage relationships of the modules were measured under the same solar spectrum as that for the simulation, i.e., the AM1.5 solar spectrum using a solar simulator (WXS-1555-L2, WACOM). The modules were set on a bench so that the center of the modules were located at a certain distance from the aperture of the solar simulator. In this case, the influence of the difference in the intensity depending on the locations in a cell can be neglected.

Relative short-circuit current density (J_{sc}(relative)), i.e., the short-circuit current density normalized by the value for the standard module was used as a measure for the evaluation and compared to the simulated results. It was calculated by the following expression.

$$J_{sc}(\text{relative}) = \frac{I_{sc}/A}{I_{st}/A_{st}}$$

where I_{sc} and A are the short-circuit current and projective area of a measured module, respectively, and I_{st} and A_{st} are the values of the standard module ($\theta = 0^\circ$ (horizontal arrangement), Cell number $= 1$, no mirrors).

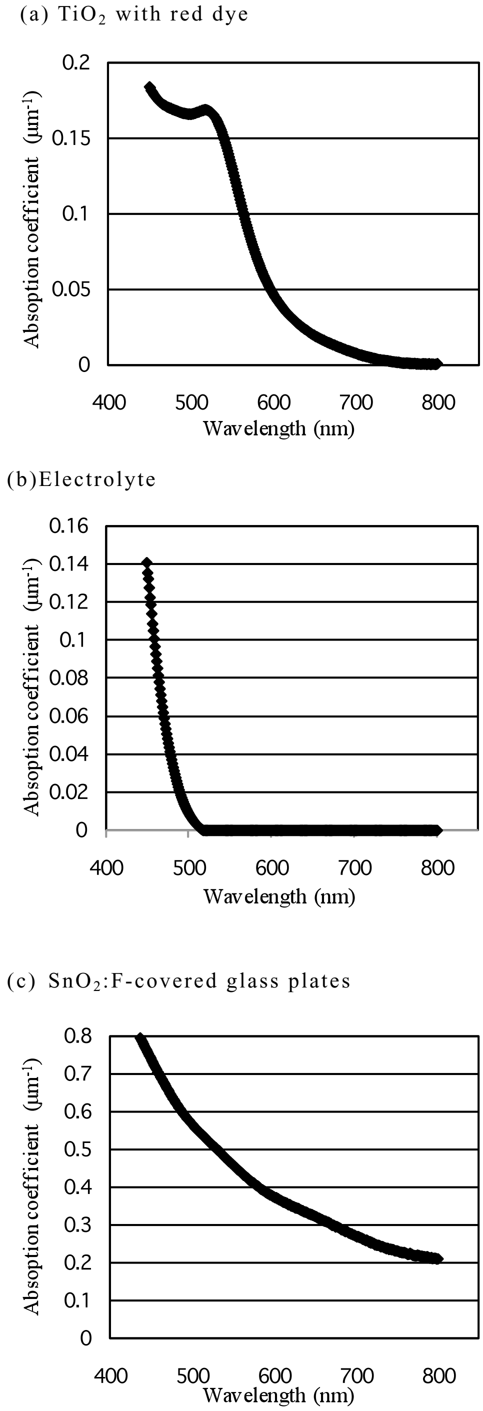

Fig. 5. Optical constants of the materials. (a) TiO_2 with red dye, (b) electrolyte, (c) SnO_2:F-covered glass plates.

5. Results

Figures 6 and 7 show the results of the simulation. The dependence of J_{sc}(relative) on the inclination angle of the cells (θ) for three kinds of the cell number in a module (N_{cell}) is shown in Fig. 6, where $\theta = 0^\circ$ stands for the horizontal arrangement. The optimal angle to achieve high conversion efficiency shifts to a lower side with increasing N_{cell}; e.g., 70° for $N_{cell} = 1$ and 50° for $N_{cell} = 10$.

The influence of N_{cell} is more apparently shown in Fig. 7. When θ equals 30°, J_{sc}(relative) rapidly increases with increasing N_{cell} up to 10 and still gradually increases up to $N_{cell} = 100$.

The rapid increase in J_{sc}(relative) is also found at $\theta = 50^\circ$. However, after showing the maximum being 118% with $N_{cell} = 10$, J_{sc}(relative) rapidly decreases with increasing N_{cell}. The optimal N_{cell} is fewer at $\theta = 70^\circ$; the maximal J_{sc}(relative) is 115% with $N_{cell} = 3$.

The dependence on θ mentioned above is shown in more detail in Fig. 8, with experimental data. The optimal θ obtained by the present simulation are in good agreement

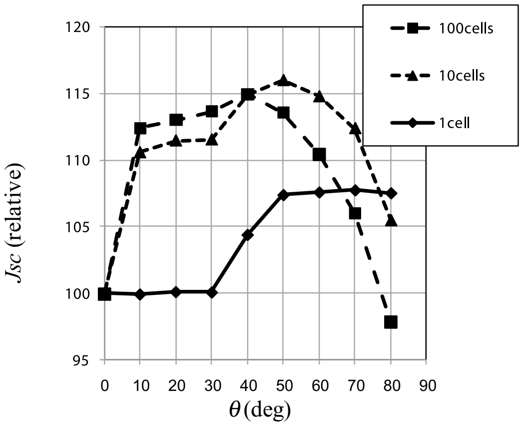

Fig. 6. Calculated J_{sc}(relative) as a function of θ.

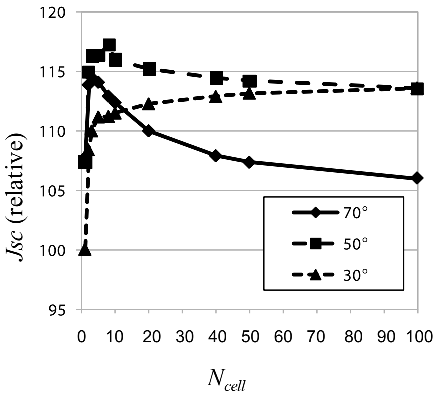

Fig. 7. Calculated J_{sc}(relative) as a function of N_{cell}.

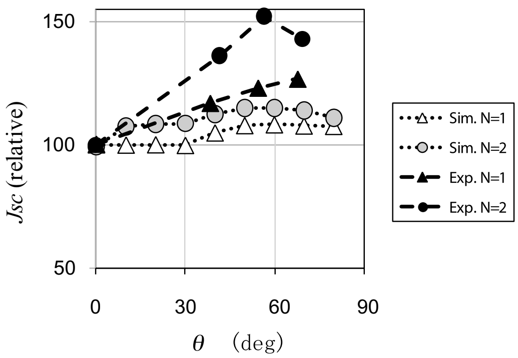

Fig. 8. Comparison of the results of the simulation and experiments.

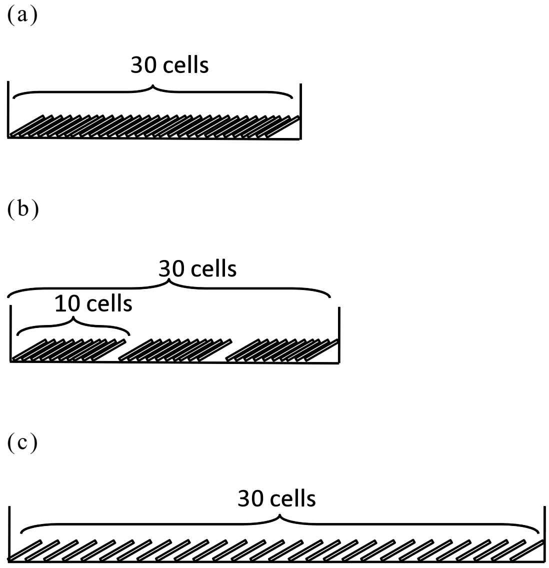

Fig. 9. Arrangements of practically large-sized modules using 30 cells with $\theta = 40^{\circ}$.

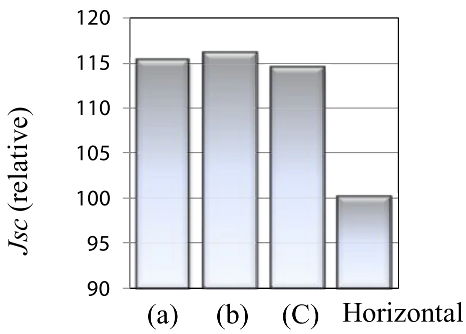

Fig. 10. Comparison of J_{sc}(relative) of the three arrangements shown in Fig. 9.

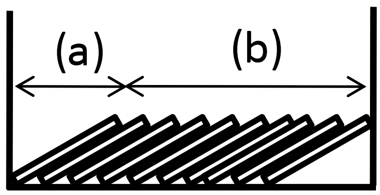

Fig. 11. Difference of the incident locations of the rays. (a) Upper surface, (b) cross-sections.

with the experimental values for each N_{cell} value. The experimentally observed highest J_{sc}(relative) was 150% at $\theta = 56^{\circ}$, $N_{cell} = 2$, that is considerably higher than the simulated value being 118%.

Arrangements for practically large-sized modules were evaluated by the simulation. Figure 9 illustrates three arrangements of the modules using 30 cells. The comparison of the resultant J_{sc}(relative) to that for the horizontal arrangement is shown in Fig. 10. The most significant improvement was achieved using Arrangement (b): by 16%. It is worth noting that J_{sc}(relative) of Arrangement (b) is a little higher than that of Arrangement (a), although the cell number per unit area in Arrangement (b) is fewer. This is practically of a great advantage for module cost reduction. The cell number per unit area can be significantly decreased by using Arrangement (c), with maintaining the J_{sc}(relative) value close to those of Arrangement (b). Therefore, this arrangement would provide the best cost-performance.

6. Discussion

The optimal value of N_{cell} depends on θ. This is due to the fact that the areal ratio of (a) and (b) shown in Fig. 11, where the light is incident from the upper surfaces and from the cross-sections, respectively, depends on both N_{cell} and θ.

As for the incident light from the upper surface (area (a) in Fig. 11), the absorbance increases with increasing N_{cell}, because the light that passes through the first cell can be absorbed in the second cell, third cell, etc. The absorbance for the light incident from the cross-sections is lower than that from the upper surfaces on average, because considerable portion of the light is multiply reflected at the interfaces between the glass/air and glass/absorbing layer in the cells, i.e., propagates in the glass plates like a guided wave, and hence penetrates into the absorbing layers only slightly. This fact decreases the total absorbance with further increasing N_{cell}.

The optimal N_{cell} is determined from this trade-off relation. The effect of increasing absorbance for area (a) is more significant at a smaller θ, resulting in the larger optimal N_{cell} as shown in Fig. 7. In the right-side edge in area (b), the cells are not sufficiently stacked. Such an area, in which the absorbance is lower, accounts for only a small fraction of the total area, and it has been confirmed by the simulation that the influence of the lower absorbance is negligibly small.

It was experimentally observed that J_{sc}(relative) was improved by up to 50% by changing the arrangement of the cells in a module. However, this value is considerably higher than the result of the simulation: 15%. There are three possible reasons of the difference between the experimental result and simulated one.

The first is the fact that the cells used in the experiments are not of an exactly rectangular shape. The influence of the shape was roughly estimated to cause overestimation of around 5% (relative). Therefore, if the actual shape is involved in the simulation, the improvement would be around 20%.

The second is inaccuracy of the optical constants used in the simulation that could not be negligible. It is difficult to measure rather low values of the absorbance in the long wavelength range with sufficient accuracy. Meanwhile, the effect of inclination of the cells is more significant in the long wavelength range, and hence the inaccuracy of the measured values would affect considerably on the resultant J_{sc}(relative). Using the absorbance being the half of the measured value, the simulation provides 30% improvement in J_{sc}(relative).

The last reason is caused by the fact that the incident light rays emitted from the solar simulator are not perfectly collimated. When the cells are inclined in a module, non-collimated components of the incident lighet is reflected on the bottom mirror to the back sides of the cells. This results in an incident light intensity a little higher than that for the standard modules. Meanwhile, perfectly parallel rays used in the simulation ensure the same intensity for all the arrangements of the modules. Therefore, the improvement under the sun irradiation in reality, which provides perfectly parallel rays, is likely a little lower than the values achieved in the present experiments.

7. Concluding Remarks

We have revealed that the performance of photovoltaic modules using thin film solar cells can be improved by 15–50% by optimally arranging the solar cells in the modules, by both simulation and experiments. The most significant improvement was achieved by appropriately arranging bundles that consist of several cells inclined with respect to horizon.

When the cells are optimally arranged in a module, the electricity per unit area of the cells is around 80% compared to the horizontal arrangement. Nonetheless, with considering the appreciable costs of the other parts in the modules: frames, fillers, etc., the results of the significant increase in the conversion efficiency of the modules suggest that the method presented here improves the cost performance (low ¥/kWh) of the modules. Lower system costs can also be achieved, because the module cost accounts for a substantial fraction of the system cost: 40–60%. Dye-sensitized cells and organic cells, that could realize much lower costs among thin-film cells, are more suitable to be applied to the present method.

References

Fillinger, A. and Parkinson, B. A. (1999) The adsorption behavior of ruthenium-based senstizing dye to nanocrystalline TiO_2, *Journal of The Electrochemical Society*, **146**, 4559–4564.

Green, M. A., Emery, K., Hishikawa, Y. and Warta, W. (2009) Solar cell efficiency tables (version 33), *Progress in Photovoltaics*, **17**, 85–94.

Kao, M. C., Chen, H. Z., Young, S. L., Kung, C. Y. and Lin, C. C. (2009) The effects of the thickness of TiO_2 films on the performance of dye-sensitized solar cells, *Thin Solid Films*, **517**, 5096–5099.

Kusama, H., Kurashige, M., Sayama, K., Yanagida, M. and Sugahira, H. (2007) Improved performance of Black-dye-sensitized solar cells with nanocrystalline anatase TiO_2 photoelectrodes prepared from $TiCl_4$ and ammonium carbonate, *Journal of Photochemistry and Photobiology*, **189**, 100–104.

NREL (U.S.) ASTM G173-03 Reference Spectra Derived from SMARTS v. 2.9.2, <http://rredc.nrel.gov/solar/spectra/am1.5/ASTMG173/ASTMG173.html> (29 October 2009).